Integration of Well Logs and Seismic Data for Development of RasKanayes Field, North Western Desert, Egypt

El-Masry M.M.I.[1], Shendi El.H.[1], Afify W.[2] and Beshta S.M.[2]

[1]Geology Department, Faculty of Science, Suez Canal University, Ismailia, Egypt
[2]Khalda Petroleum Company, Cairo, Egypt
Samy.Beshta@khalda-eg

Abstract: The Upper Safa sandstone forms an important hydrocarbon reservoir in the RasKanayes field, North Western Desert of Egypt. The aim of this work is to demonstrate the effect of Upper Safa reservoir petrophysical characteristics and subsurface structures on the development of RasKanayes field, through the intensive integration between seismic and petrophysical analyses. The seismic interpretation shows that the structure of Upper Safa reservoir, as indicated by seismic sections, forms a tilted- fault block separating the area into two compartments. The first one is considered the main structure in the RasKanayes field, and is represented by faulted, four-way dip closure bounded by a series of normal faults. The second is located to the east of the study area, and extends in the NNE-SSW fault - trending structure. Four well logs have been analyzed and mapped, using the Petrel and Interactive Petrophysics (IP) softwares, to determine the lithological constituents and fluid saturations of the Upper Safa reservoir. Maps and cross sections, from seismic and well logging data, were used to explain the impact of geological structure in the development of the study area. RasKanayes field has high porosity and hydrocarbon saturation values due to the extensive fracturing in the field caused by faulting and folding. This was supported by the high structural position, good porosity, low shale content, low water saturation and a high percentage of hydrocarbon saturation. This encourages drilling more development and exploratory wells in northeast and central parts of the study area to enhance productivity in the RasKanayes gas-condensate field. Consequently, integrating geological structures and accurate petrophysical evaluation of an area leads to successful development.
[El-Masry M.M.I., Shendi El.H., Afify W. and Beshta S.M. **Integration of Well Logs and Seismic Data for Development of RasKanayes Field, North Western Desert, Egypt.** *Nat Sci* 2018;16(5):130-139]. ISSN 1545-0740 (print); ISSN 2375-7167 (online). http://www.sciencepub.net/nature. 18. doi:10.7537/marsnsj160518.18.

Keywords: Seismic Interpretation, Well Logging Analysis, Reservoir Characteristics, Matruh Basin, Safa Formation, RasKanayes Field, North Western Desert.

1.Introduction

The Western Desert of Egypt covers an area of about 700.000 square Kilometers and comprises almost about two thirds of the whole area of Egypt (about 1.000.000 square kilometers). It extends 1000 kilometers from the Mediterranean shoreline in the north to the Sudan border in the south and from 600-800 Kilometers from the Nile Valley in the east to the Libyan border in the west.

The area under study (Fig. 1) deals with Raskanayes gas/condensate field (in Matruh basin) is a part of Khalda petroleum company concession, in the northern part of the Western Desert of Egypt. It lies between longitudes 27° 36' 51", 27° 44' 37" E and latitudes 31° 00' 48", 31° 06' 50" N. The Raskanayes block covers an area of 136 Square kilometers. It is located approximately 7.5 km south of Mediterranean (Fig. 1). This area is a part of the western desert which is considered the most prolific petroleum province in Egypt.

The main objectives of the present study were aims to delineate the structure elements affected the study area and determine the Upper Safa reservoir parameters characterizing the pay zone from well log data to spotlighting on the promising locations for exploration.

2. Geological setting

The Western Desert has a very varied geological history. During the period when major reservoir bodies were being deposited (Jurassic to Cretaceous, 195–65 Ma ago), the Tethys shoreline was moving across the area. As the Tethys extended southwards, coastal and tidal sandstones were deposited **(Sestini, 1984)**. At other times, the entire Western Desert region was covered by the Tethys and shells and marine carbonate mud were laid down on a sea floor. The stratigraphic column of the northern Western Desert **(Egyptian General Petroleum Corporation, 1992)** includes a sedimentary succession from the Pre-Cambrian basement to the recent strata (Fig. 2). The total thickness, despite some anomalies, increases progressively to the north and northeast areas from about 6,000 ft in the south to about 25,000 ftalong the coastal area.

The stratigraphic succession of the northern Western Desert can be subdivided into four major regressive cycles, each terminated by a marine

transgression **(Sultan and Halim, 1988)**. The earliest cycle consists of the Middle and Late Jurassic nonmarineclastics (Ras Qattara Formation). These nonmarineclastics are overlain by marine Jurassic clastics of Khatatba Formation. During the Late Callovian, shallow marine carbonates of the Masajid Formation were deposited. These represent the maximum of the Jurassic transgression. A major unconformity separates the Masajid Formation from the Alam El Bueib Formation.

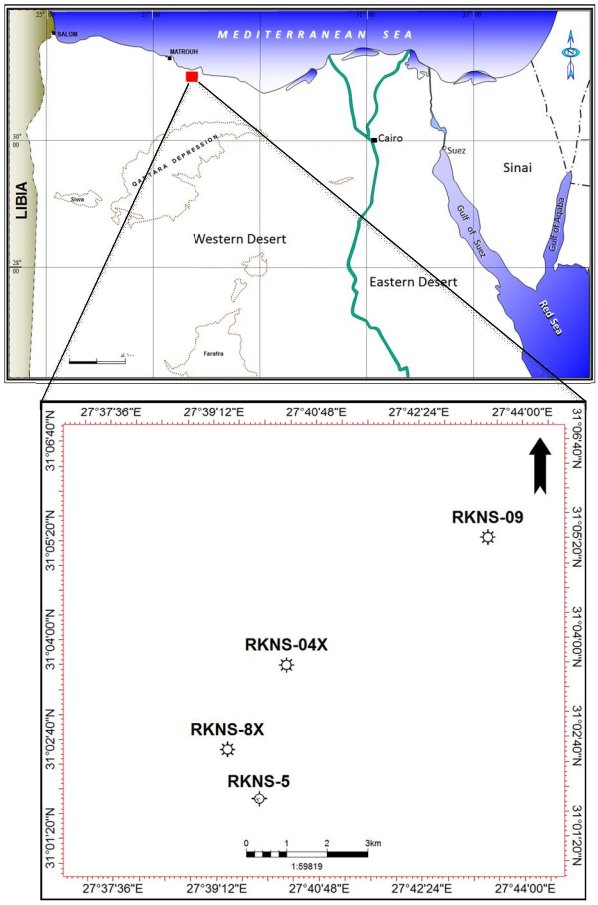

Figure1. Location Map of the study Area

The second cycle began in the Early Cretaceous with the deposition of the shallow marine clastics and carbonates of Alam El Bueib and ended with the thin Middle BarremianDahab shale. In the Late Barremian to Early Aptian times, another unconformity separated the Dahab Shale from the Kharita Formation. The third cycle extended from the Middle Albian to the Early Tertiary periods. The continental and shoreline sands of the Kharita Formation represented the initial regressive period of sedimentation. The Khoman chalk Formation was deposited in the northern Western Desert, and it was frequently bounded by unconformities, with the eroded Turonian below and the Eocene Apollonia Formation above. The final cycle consisted of the Dabaa and Moghra marineclastics, which were capped by the Marmarica limestone. The flat-lying Marmarica was found at the surface in many parts of the northern Western Desert **(Zein El-Din et al., 2001)**.

In the northern part of Western Desert (unstable shelf area), the lithostratigraphic column may be subdivided into three sequences. First the lowerclastic unit (sandstone and shale), from Cambrian to Cenomanian, second the middle carbonates, from Turonian to Eocene and finally the upper clastic unit (sandstone and shale), from Oligocene to Recent **(Metwalli et al., 2007; Said, 1962)**. Khatatba Formation (Safa and Zahra) is Middle Jurassic; it is represented transitional facies from Bahrein and Wadi El-Natrun formations. It is composed of shale, sandstone and some carbonate in the northeast, which grades upwards into the Masajid limestone. In the south and west, carbonaceous shale, coal, marine shale, siltstone, fine sandstone and red shale (Yakout bed) occurs at the base **(Norton, 1967; Hantar, 1990)**. Khatatba Formation contains some fair to excellent quality oil–prone source rock (type II kerogen) with gas-prone humic organic matter (type III) in most parts of the Western Desert. The source rocks are generally rich and mature **(EGPC, 1992)**. **Said (1962)** classified the Western Desert into three major tectonic units. The tectonic features of these unite, from south to north, are reviewed, as follows (Fig. 3):

1) The stable shelf occupies the southern area of Western Desert, south latitude 28° 00" N. It is characterized by high basement relief, exposed to the south (Gabel Owienat). Thin sedimentary cover of mainly Mesozoic fluvial-continental clastics section overlies these basement rocks.

2) The unstable shelf is located directly north of the stable shelf. It is characterized by the northward thickening of the sedimentary section underlain by low basement relief. The sedimentary section in this area reaches thousands of meters in thickness and is of Paleozoic to recent in age. It is characterized by high organic richness, faulting and folding geometry which favorable for hydrocarbon accumulations. All or most of oil and gas fields have been located in this shelf.

3) The hinge zone is very narrow in width and is parallel to the Mediterranean Sea coast to the south. It is the area lying between Miogeosyncline and unstable shelf. It is responsible for the rapid thickening of Oligocene to Pliocene sediments that forming the Nile delta to the north. The Miogeosyncline unit is occupied by the present day Mediterranean Sea and Nile Delta. It is very thick Tertiary sedimentary section.

The study area belongs to the unstable shelf of the North Western Desert. The general history of the area, which is a part of the unstable shelf history, is

related to the tectonic regimes that affected northern Egypt. These regimes were also responsible for the formation of basins and sub- basins and influence to great extent their depositional framework.

3. Seismic Interpretation

The available data for the current study are complete electric logs for four wells and 2D seismic lines, courtesy of Khalda Petroleum Company, Egypt. To achieve the goal of this study, the following processes were applied to the available data: seismic well tie, picking horizons and structural features, velocity maps, depth conversion, depth contour maps. Seismic interpretation involves tracing and correlating along continuous reflectors throughout the 2D dataset which are used for the geological interpretation. The aim of this is to produce structural maps that reflect the spatial variation in depth of certain geological layers.

3.1 Seismic well tie and reflectors identification

Well control is an essential for the successful interpretation of seismic sections; but, when available, it is an invaluable aid to the interpreter **(Badley, 1985)**. It provides the link between lithology and seismic reflections and stratigraphic calibration of seismic sequence boundaries. Synthetic seismogram gives the interpreter confidence in horizon picking, correlation, and time-depth relationship and allows interpreter to identify multiples in the seismic data.

Generation of the synthetic seismograms was performed using Petrel Software. In creating a synthetic seismogram, Petrel software permits the interpreter to tie time data (the seismic data) to depth data (the well data) by integrating over the velocity profile. Impedance log and reflection coefficients are generated from the velocity and density profiles. Using the sonic and density log combinations available for a particular well, a wavelet is convolved with the reflection coefficient to create a synthetic seismic trace.

In the current study, synthetic seismograms for all wells which passed through or near seismic lines were constructed using broad band zero phase wavelets extracted from the seismic data.

the synthetic seismogram constructed for well (Ras Kanayes-4X) shows a good tie to seismic data particularly at the time zone of interest (Fig. 4). Generally, the tie between this synthetic seismogram and the seismic data is satisfactory. The main objective of synthetic seismogram is also to make time-depth relationship. Consequently, two-way times are calculated and used to define the reflecting formation tops on the seismic sections. The Safa Formation is the most powerful event on the seismic sections and exhibits the best continuity. The markable tops of the Upper and lower Safa is selected to show the development of structural elements affecting the Jurassic rock units.

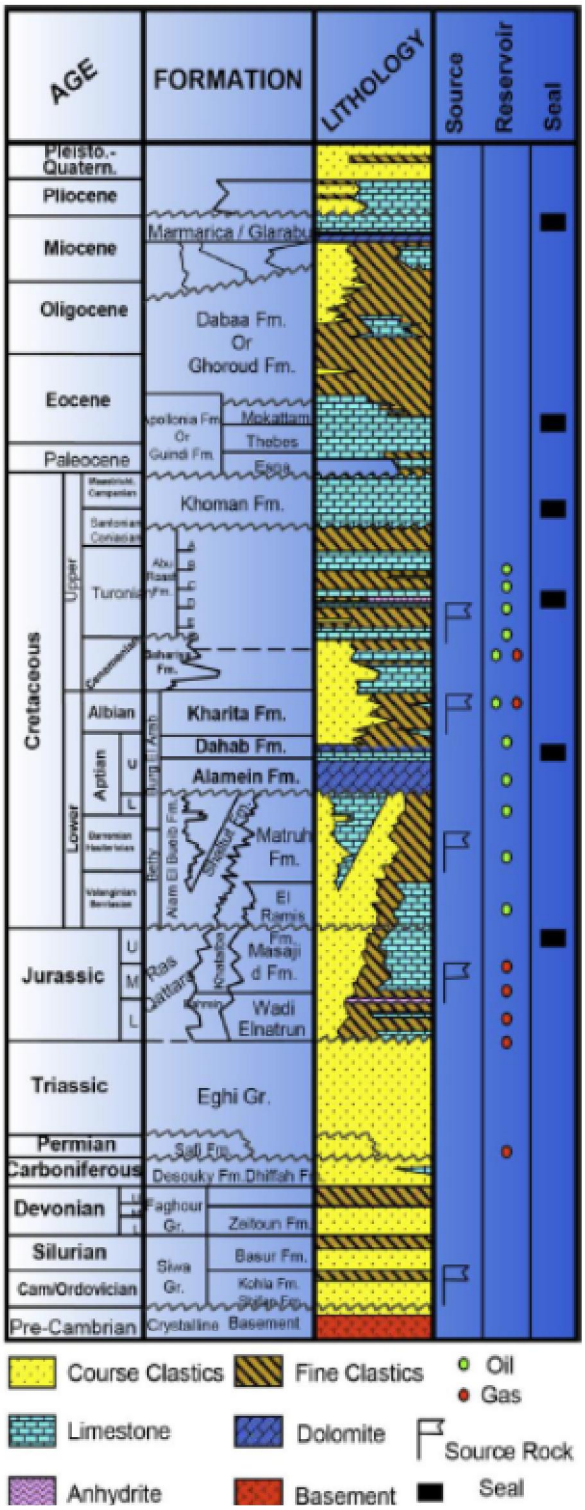

Figure 2. Generalized Litho-Stratigraphic Column of Western Desert (EGPC 1995).

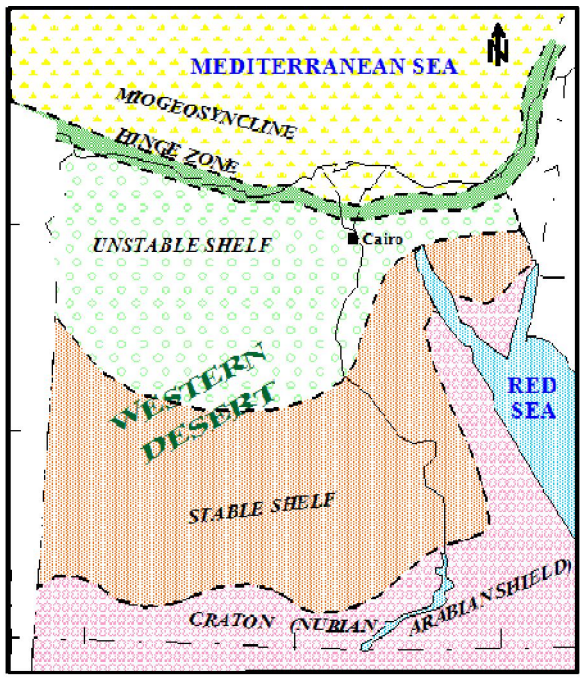

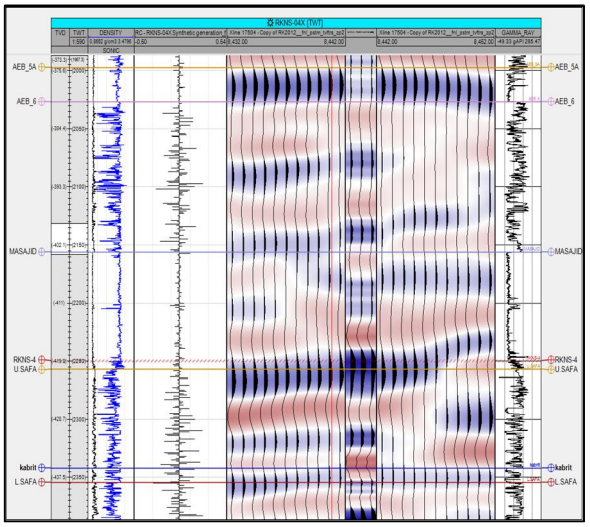

Figure4. Synthetic seismogram for (Ras Kanayes-4X) well andits seismic tie.

3.2. Picking horizons and structural features

One simply traces the particular reflector on a series of seismic lines which intersect perpendicular in planar view, culminating with a product that correlates on every line. By correlating specific horizons on a seismic line, one may subsequently generate time data which, after conversion to depth, help generate structural maps (maps which show the geologic structure of a feature) and isochron or isopach maps (maps which show time or thickness of particular intervals, respectively).

Based on the seismic well tie the interpret horizons were chosen in the seismic data. The main attention was focused over the reservoir interval, where two horizons were selected to interpret. The selected two horizons for interpretation are Upper Safa and Lower Safa (Figs. 5 and 6). Fault planes and their intersections with horizons were digitized from the screen display in a similar way as horizons picking. Fault intersections can be marked by special symbols on a base map. These make it easy for interpreter to keep track of what lines have been interpreted and the emerging structural map.

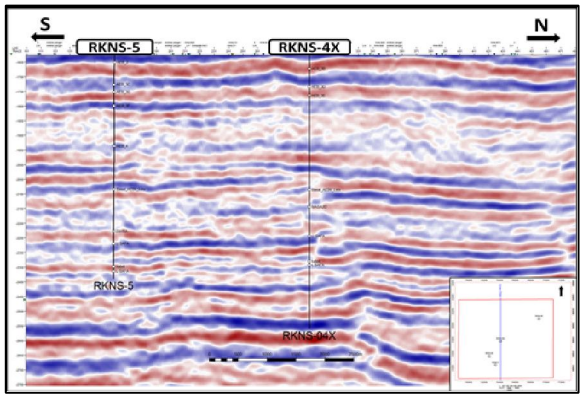

Figure5. Un-interpreted seismic line passing through RKNS-4X well

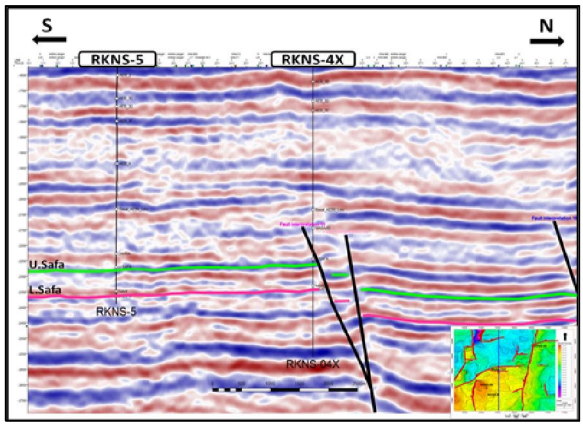

Figure6. Interpreted seismic line passing through RKNS-4X well

Because of the fault roles in the entrapment of hydrocarbons, the techniques for finding and mapping faults have considerable importance. The principal indications of faulting on reflection sections are the following **(Dobrin and Savit, 1988)**:

1. Discontinuities in reflections falling along an essentially linear pattern.
2. Divergences in dip not related to stratigraphy.
3. Diffraction patterns, particularly those with vertexes that line up a manner consistent with local

faulting.

4. Distortion or disappearance of reflections below suspected fault lines.

3.3. Construction of the Upper Safa Horizon

3.3.1 Construction of time structure map

The given seismic data are analyzed primarily in terms of structural elements. This is currently achieved through the picking of seismic reflection horizons of interest and the definition of the operated structural elements. Correlation of seismic events, tying their times, closing their loops, posting their time values and fault segments, constructing the fault pattern and contouring the arrival times are the basic steps followed for seismic interpretation **(Coffeen, 1984)**. Accordingly, the fault cut-outs are picked and posted on their locations on the seismic shot point base map to establish the fault pattern for the concerned top. Also, the two-way time values are transferred to their location on the map and contoured to construct the time structure contour map on the top of the formation.

The picked time values and the locations of fault segments are posted on the base map of the study area in order to construct 2D structure maps at the top of Upper Safa horizon (Fig. 7). The two-way-time of the Upper Safa varies between -2235.8 to -2449.7 ms.

3.3.2. Average velocity map

The average velocity (V_{av}) is simply defined as the velocity over certain reflecting surface below the seismic reference datum **(Dobrin, 1976)**.

$V_{av} = Z/T$

Where;

Z= the depth to the reflecting surface from the wells in ft, and

T=the one-way transit time to the reflector from the same reference in ms.

The average velocity map of the Upper Safa shows that, the velocity range at this level is 11647.13 – 11941.39 ft/s. (Fig.8).

3.3.1 Construction of depth structure map

The time structure and average velocity maps are used to convert the reflection times to depths, in order to construct the depth structure contour map (Fig. 9). The depth structural contour map shows the structural elements in terms of depth rather than time. The depth values of Upper Safa vary between -13282 and -14413 ft (TVDSS). The Northern Western Desert is subjected to two major intersecting faults, one trend NE-SW related to Jurassic rifting, and the other trends NW-SE related to late cretaceous rifting **(EGPC, 1992)**.

Raskanayes field located in Matruh basin which is dissected by NE-SW oriented faults. These observations indicate a phase of Jurassic - Early Cretaceous rifting, the study area created in Jurassic due to Early Jurassic plate movement including opening of Neotethyes and inverted in Late Cretaceous due to strike slip movement which is caused by compressional force of Syrian Arc movement **(Moustafa, 1999)**.

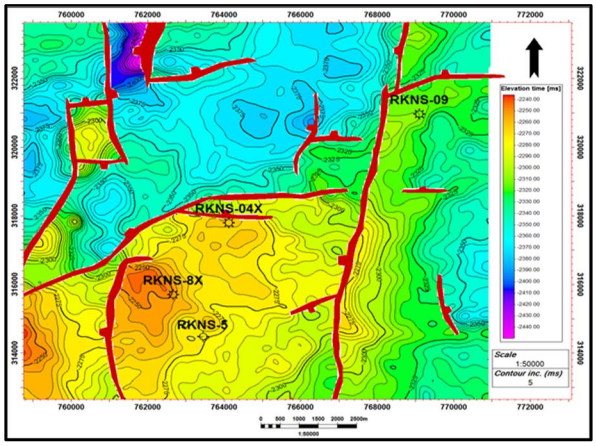

Figure 7. Time structure map on the top of Upper Safa horizon.

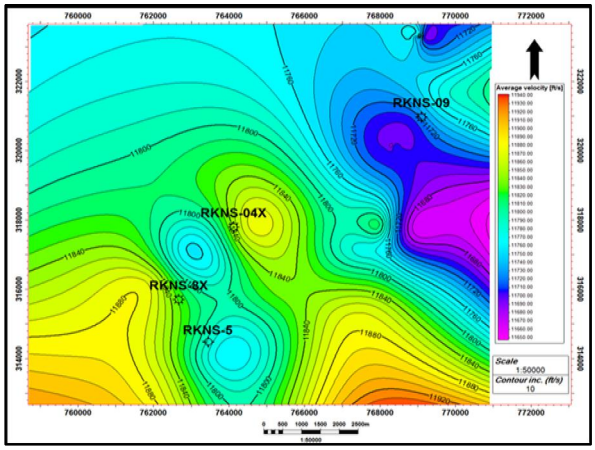

Figure8. Velocity map of the Upper Safa horizon

The depth map of Upper Safa unit shows that the study area is controlled by two major tectonic events which affected on the configuration of fault pattern. There are two main directions of faults inferred from map, East-West direction faults corresponding to Pre-Cambrian to Palaeozoic tectonic movement of North Africa and Northeast-Southwest direction represents normal fault and these major faults are the most dominant in the area and corresponding to Jurassic rifting movement of North Africa. the structure of Upper Safa reservoir forms a tilted fault block separating concerning area into two compartments; 1st one is considered the main structure in the RasKanayes field, which represented by faulted four way dip closure bounded by a series of normal faults. 2nd structure located in the eastern direction of the studied area, extended from north to the south belonging the NNE-SSW fault.

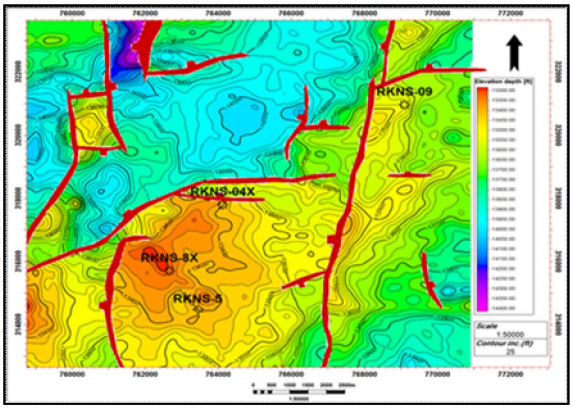

Figure 9. Depth map of the Upper Safa horizon

4. Petrophysics and Formation Evaluation

A suite of logs from four wells in the area (Fig. 1) was provided by Khalda Petroleum Company, including gamma-ray (GR), spontaneous potential (SP), density, neutron, caliper, and resistivity, however only one well have sonic log. Well logs have been successfully used in exploration and development wells as a part of drilling practice, to provide more information and greater accuracy of reserve evaluation **(Connolly 1965; Brown 1967)**, the depth and thickness of productive zones. Additionally, they are used to distinguish between oil, gas and water in reservoir and to estimate hydrocarbon reserves **(Asquith and Krygowski, 2004)**.

4.1 Lithology identification

A lot of ways is used to determine lithology, from logs using different types of crossplots. These crossplot combinations were discussed in **Poupon and Leveaux (1971); Schlumberger (1974) and Dresser Atlas (1979)**. The crossplots of binary and tri-porosity logs are convenient to display both porosity and lithology information. The crossplots used in this work are:

4.1.1 Density - Neutron crossplot

The cross plots used in this work are the Neutron-Density crossplots. The Neutron-Density cross plots are commonly used to determine the lithology (using the neutron and density logs) and accurately evaluate the matrix porosity of carbonate rocks. The effect of light hydrocarbons (gas) can be observed on the cross plot, where the plotted data tend to shift north-westerly from the limestone line, since this effect increases porosity determinations from density log and decreases neutron porosity. Also, the effect of shale can be observed on the cross plot, where the shale effects tend to be in the southeast quadrant of the cross plot **(Poupon and Leveaux, 1971)**.

The density-neutron crossplot performed for Upper Safa sand reservoir for each well in our study, for example Figure 10 shows the Density-Neutron crossplot that have been applied to the upper Safa sand reservoir of the Ras Kanayes-4X well. It is observed that the majority of plotted points are located on sandstone line and in between sandstone and limestone lines with porosity ranging from 7% to 15%. This indicates that the reservoir is mainly sandstone with calcareous cement. The effect of gas is observed where some points are shifted upward above sandstone line.

4.1.2 M-N crossplot

Mineralogical interpretation with neutron, density, and sonic logs is facilitated by the use of M-N crossplot which reflect the lithology types. This plot was first introduced by **Bruke et al. (1969)**. The effect of secondary porosity, shaliness, and gas-filled porosity will shift the position of the points with respect to their true lithology, and can even cause the M-N points to plot outside the triangular area defined by the primary mineral constituents. The displacement of the plotted points upward indicates secondary porosity while the effect of gas may shift the points upwards on the right. No unique shale point exits on the M-N plot because shales tend to vary in their characteristics. Mostly, shale effect will be situated below the line that joins the silica and anhydrite points **(Bigelow, 1995)**.

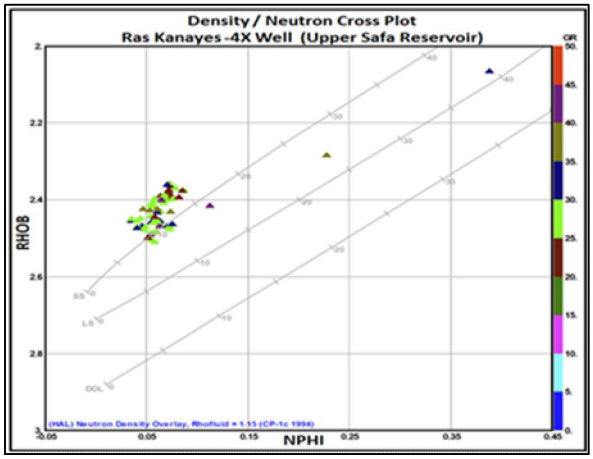

Figure10. Ras Kanayes-4X Well Density neutron crossplot of the Upper Safasand reservoir.

The M-N crossplot which performed on the Upper Safasand reservoir for Ras Kanayes-4X well, (Fig. 11) shows the mineralogical composition of the Upper Safa reservoir in Ras Kanayes-4X well. The majority of the plotted points are tending to be close to quartz region. This may reflect the presence of clean sandstone reservoir. Moreover we can note that some points shifted upward due to gas effect and secondary porosities.

4.2 Distribution of petrophysical parameters of the

study area

After calculating the values of the log-derived parameters for the Upper Safa reservoir, it is required to average and map these parameters to represent their general distribution throughout Upper Safa reservoir. **Table 1** shows the reservoir parameters which were derived from average calculations of different log parameters.

4.2.1 Vertical distribution of petrophysical parameters

The vertical distribution of petrophysical parameters and lithology is presented in the form of litho-saturation Cross Plot. This Cross Plot is responsible for the formation analysis which represents the vertical distribution of rocks (lithology), fluids and porosity (total and effective porosity). Also, the digram illustrates the log package on the well from left to right (first track gamma ray, resistivity, density / neutron, pay / reservoir flag, water / hydrocarbon saturation, effective / total porosity and the last track is lithology).

Generally the vertical analysis reflects the upper safa reservoir mostly consists of a mixed lithology of sandstone, siltstone, shale and some streaks of limestone (Fig. 12). For example the vertical analysis of Upper Safa reservoir in Ras Kanayes-4X well, where the thickness of the reservoir is 580 ft, the groth sand 42.5 ft and the analysis reflect that the sand become mature in middle part of upper Safa reservoir. The middle part is characterized by the presence of considerable hydrocarbon saturation reaching to 74%. The average effective porosity is 11.3%, therefore the productivity expected from the middle sandstone zone in the formation.

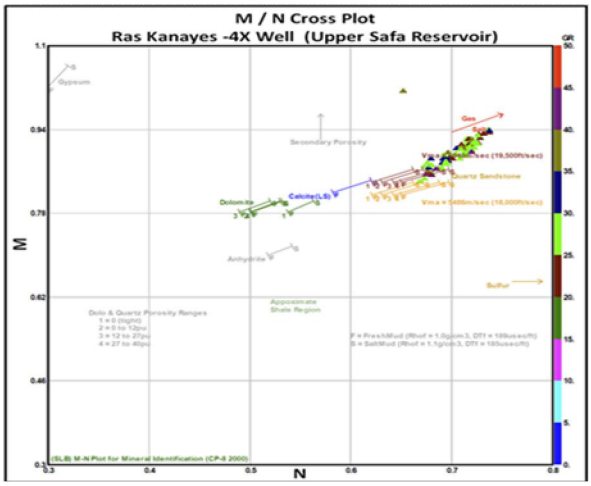

Figure11. Ras Kanayes-4X Well M – N crossplot of the Upper Safa sand reservoir.

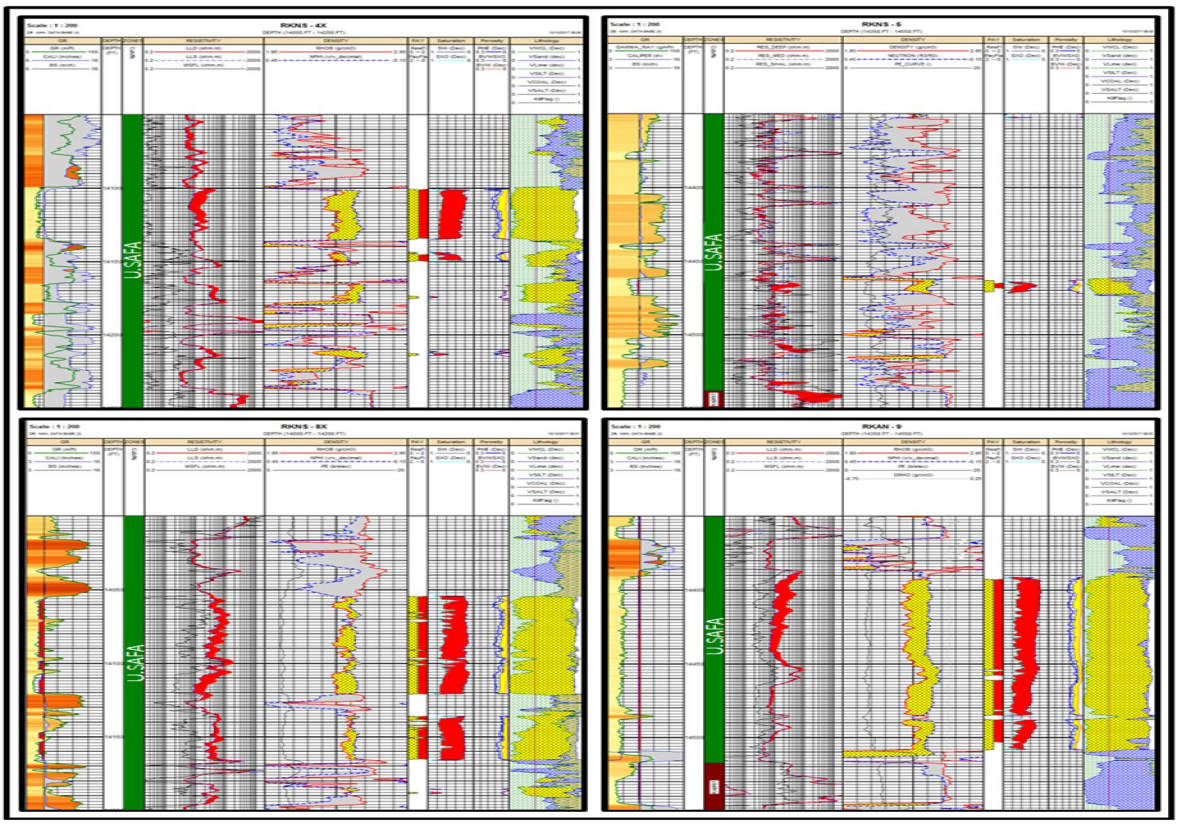

Figure12. Litho-saturation crossplots of Upper Safareservoirfor RasKanayes–4X, 5, 8X and 9 wells

Table 1. Well Log parameters of the Upper Safa reservoir, RasKanayes Field, Western Desert, Egypt.

WELL	Reservoir	Total thickness (ft)	Total porosity (%)	Effective porosity (%)	Shale volume (Vsh, %)	Gross sand (ft)	Net pay (ft)	Net / Gross (N/G, %)	Flushed Zone Saturation (SXO, %)	Water Saturation (Sw, %)	Hydrocarbon Saturation (Sh, %)	Residual Hydrocarbon Saturation (Shr, %)	Movable Hydrocarbon Saturation (Shm, %)
RKNS - 4X	U. SAFA	580.0	12.9	11.3	6.9	42.5	38.0	89.4	74.6	26.0	74.0	25.4	48.6
RKNS - 5		569.0	11.6	8.8	8.8	10.5	5.5	52.4	53.3	28.5	71.5	46.7	24.8
RKNS - 8X		597.5	10.5	9.2	10.3	87.5	87.0	99.4	65.9	16.9	83.1	34.1	49.0
RKNS - 9		647.5	12.5	10.6	5.6	113.0	103.0	91.2	72.8	30.0	70.0	27.2	42.8

4.2.2 Horizontal distribution of petrophysical parameters

The horizontal distribution of petrophysical parameters are achieved by construct the isoparametic maps of the study area. The mapping includes Upper Safa reservoir of different four wells in the study area (Ras Kanayes-4X, Ras Kanayes-5, Ras Kanayes-8X and Ras Kanayes-9).

The shale volume distribution map of the Upper Safa reservoir (Fig. 13) shows that the shale volume attains its lowest value of 5.6 % at Ras Kanayes-9 well and highest value of 10.3% at Ras Kanayes-8X well. The shale volume content decrease almost in the central part of the study area and the north eastern direction, while it increases in the north western and south eastern directions.

The gross sand distribution map of the Upper Safa reservoir (Fig. 14) shows a marked increase all over the area especially from the middle to the west and in the north eastern directions, with the maximum value of 113 ft at Ras Kanayes-9 well and it decrease in the south and eastern south directions, with minimum value 10.5 ft at Ras Kanayes-5 well.

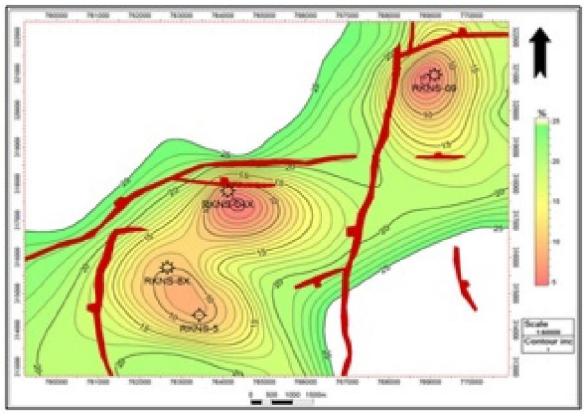

Figure13. Shale volume map of the Upper Safa reservoir.

The effective porosity in the Upper Safa reservoir increase toward the northeastern corner and in the central part of the study area to reach the maximum value 11.3% at Kanayes-4X well, while it decreases in the southwest, north and southeastern directions of the study area, where it reaches the minimum value 8.8% at Ras Kanayes-5 well (Fig. 15).

The net pay distribution map (Fig. 16) of the Upper Safa reservoir shows an increase in north east and in central part of the study area. It reaches maximum value of 103 ft at Ras Kanayes-9 well and decreases toward the northwest, east and south directions of our *study area. The minimum value reaches to 5.5 ft at Ras Kanayes-5 well.*

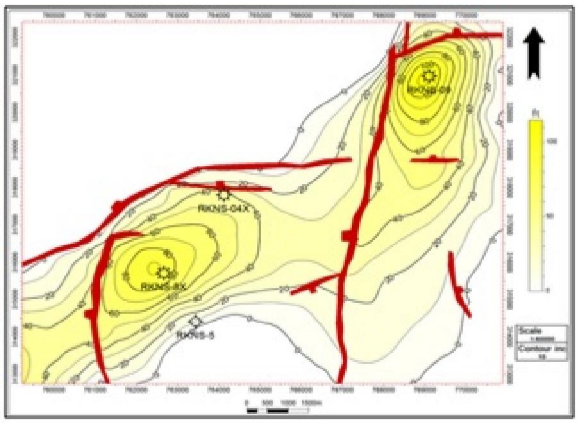

Figure14. Gross sand map of the Upper Safa reservoir.

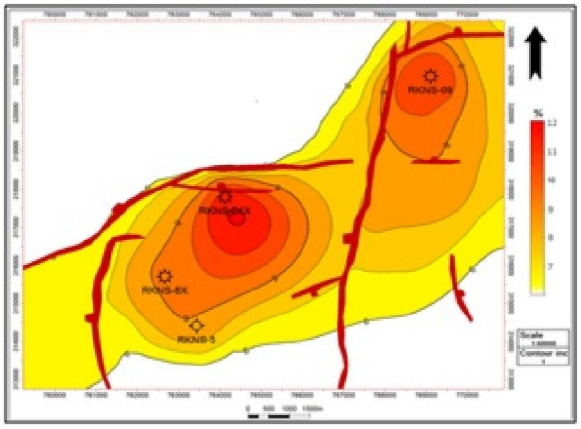

Figure15. Effective porosity map of the Upper Safa reservoir.

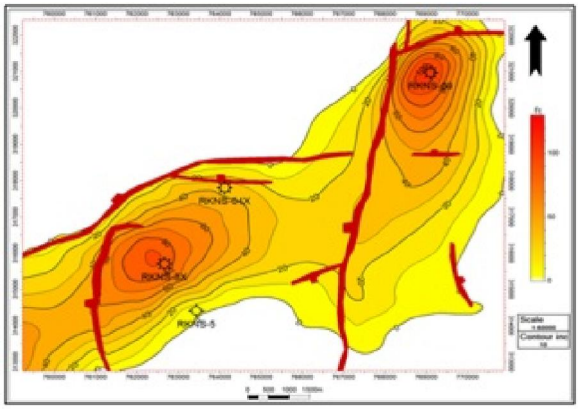

Figure16. Net pay map of the Upper Safa reservoir.

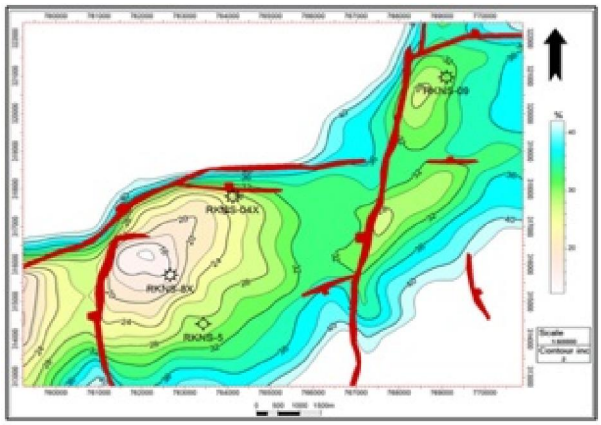

Figure17. Water saturation map of the Upper Safa reservoir.

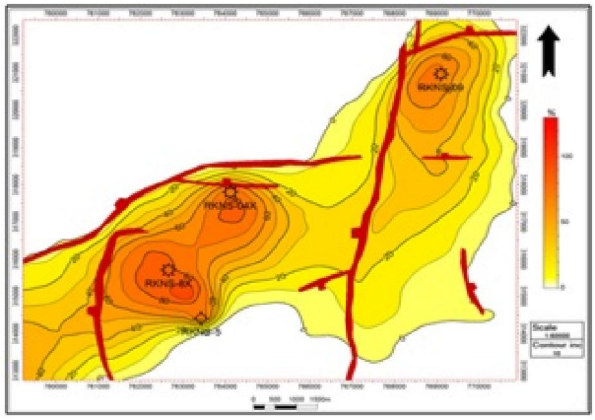

Figure18. Hydrocarbon saturation map of the Upper Safa

The water saturation distribution map of the Upper Safa reservoir in the study area (Fig. 17) shows a remarkable increase in the central part of the study area extended to southwestern and northeastern directions, where it reaches maximum value of 30% in Ras Kanayes-9 well. The water saturation decreases in south, southeastern, north and north western directions where it reaching the minimum value of 16.9 % at Kanayes-8 well.

The hydrocarbon saturation map (Fig. 18) of the Upper Safa reservoir illustrates a decreasing value toward south, northwest and east directions of the study area, where it reaches minimum value of 70% at Ras Kanayes-9 well. The map shows increase in northeast and in the central part of the study area where, the maximum value is 83.1% at Ras Kanayes-8X well.

5. Conclusion

The Upper Safa reservoir is comprehensively described and analyzed in thisstudy area. The hydrocarbons are accumulated inthe trap has the forms of faulted four-way and three-way dip closurestructures. Some ofthe trapping structures could have possibly beencharged by hydrocarbons. Accordingly, by integrating the seismicinterpretation with the results of Petrophysicalparameters analysis, it can be concluded that thehydrocarbons potentiality of the Upper Safa reservoir was enhanced towards the northeast and in the central part of the study area. This wassupported by the high structural position, goodporosity, low shale content, low water saturationand a high percent of hydrocarbon saturation. This encourages drilling more development andexploratory wells in northeast and central partsof the study area to enhance productivity in the Ras Kanayes gas-condensate field.

Acknowledgements

We wish to express our gratitude to the Egyptian General Petroleum Corporation (EGPC) and Khalda Petroleum Company (KPC) for their permission to publish this paper.

References

1. Asquith, G.B., Krygowski, D., and Gibson, C. R. (2004): Basic well log analysis. Tulsa, Oklahoma: American Association of Petroleum Geologists.
2. Badley, M.E. (1985): Practical Seismic Interpretation. IHRDC Publishers, Boston, 266 p.
3. Banihasan, N., Riahi, M. A., and Anbaran, M., (2006): Recursive and Sparse Spike Inversion.
4. Bigelow, L., 1995: Introduction to wireline log analysis, western atlas international, Inc., Houston, Texas-USA.
5. Brown, A. A., 1967: New methods of characterizing reservoir rocks by well logging. Paper presented at the 7th World Petroleum Congress, Mexico.
6. Bruke, J.A., Campbell, R. L., and Schmidt, A.W., 1969: The litho-porosity crossplot. The log analyst (SPWLA), 10(6).

7. Coffeen, J.A., 1984: Interpretation of seismic data. Pennwell Publ. Co., Tulsa, Oklahoma.
8. Connolly, Edward T., 1965: Resume And Current Status Of The Use Of Logs In Production. Paper presented at the SPWLA 6th Annual Logging Symposium (Volume I).
9. Dobrin, M.B. and Savit, C.H., 1988: Introduction to geophysical prospecting: New York, McGraw-Hill, 867 p.
10. Dobrin, M.B., 1976: Introduction to geophysical prospecting Macgraw Hill. New York, 3rd Ed.
11. Dresser Atlas., 1979: Log interpretation charts. Dresser industries Inc., Houston, Texas, 107 p.
12. EGPC (Egyptian General Petroleum Corporation)., 1992: Western Desert, oil and Gas fields, a comprehensive overview. EGPC, 11th Petrol. Expl. and Prod. Conf., Cairo, 431 p.
13. Hantar, G., 1990: North Western Desert. In: Said, R. (Ed.). The geology of Egypt. A. A. Balkema, Rotterdam, Netherlands. pp. 293–319.
14. Metwalli, M.H., and ABakr, A. M., 2007: Seismostratigraphic Analysis of the Alam El Bueib Reservoir Sand, South Umbarka Area, Western Desert, Egypt", ISESCO, vol. 3, pp. 64-87.
15. Moustafa, A. R., 1999: Khalda regional project, results of phase I, Khalda Petroleum Company Internal Report, 11 p.
16. Norton, P., 1967: Rock-stratigraphic nomenclature of the Western Desert, Egypt. Int. Report of GPC, Cairo, Egypt, 557 p.
17. Poupon, A. and Leveaux, J., 1971: Evaluation of water saturation in shaly parts of Northern Egypt. AAPG, 60 (1).
18. Said, R., 1962: The geology of Egypt. Elsevier Publ. Co., Amsterdam, Oxford and New York, 277 p.
19. Schlumberger., 1974: Log interpretation manual/application, Houston, Schlumberger well services, Inc., Vol. 2.

4/24/2018